CHAPTER 4

PREPROCESSING FRAMEWORK FOR DE-NOISING AND SEGMENTATION

4.1 Introduction

The brain neuron images consist of Gaussian, salt and pepper noises that interrupt the image features which are vital for AD identification. The noise removal process is challenging for investigators. The objective is to reduce the Gaussian noise effect on brain neuron images. The wavelet transform technique is used to improve accuracy, especially in multi-resolution medical pictures. Preprocessing the brain neuron image prior to additional analysis is a vital practice that aids in eliminating the undesirable components from the original image. The noise elimination, image enrichment and rectification processes provide positive effects on the image analysis outcomes.

In this study, an image preprocessing framework is developed that includes image de-noising and segmentation. Brain neuron pictures are subjected to several de-noising methods, including DWT, as well as filter-based methods, including wiener, weighted median, adaptive, hampel, and AFHI (proposed approach). Another preprocessing task improves the image contrast by applying histogram-based image enhancement. These methods enhance the image quality and aids as a vital foundation for consequent classification tasks. Additionally, image segmentation strategies were implemented to enhance the image, which includes region growing, histogram based discrete wavelet transform, fuzzy set theory (FCM) and TDWT-FST (proposed technique), are applied.

This chapter is structured as follows. The following part provides a description of the image preprocessing methods, like the wiener, weighted median, adaptive, hampel, and the suggested AFHI methods for image denoising. For image segmentation, region growing, histogram-based DWT, FCM and the proposed TDWT-FST technique are presented. The performance analysis is conducted, the experimental results of these methods are examined, and the evaluations of the suggested methods are eventually

provided. These methods are applied for pre-processing brain neuron images, and the training dataset for ADNI and OASIS datasets is finally presented.

4.2 Brain Neuron Image Preprocessing Techniques

The preprocessing techniques enrich the image quality, which helps in examining the image efficiently. The preprocessing technique rejects undesirable misrepresentations and enriches the specific abilities that are important for the proposed method to work powerfully. The MRI of a brain consists of noises like speckle, salt and pepper, Gaussian and so on. Accurately obtaining a image of the brain is difficult. Classifying the stages of AD disease requires a precise brain image for further diagnosis. Preserving and preserving the necessary image information after processing to produce actual image classification is one of the main issues in the preprocessing stage. Different kinds of image preprocessing techniques such as image de-noising and image segmentation are proposed in this study.

The main focus of image processing research is MRI denoising. The image quality deteriorates during capturing, processing, and storing of the image. Hence, eliminating and reducing the noise from the original MR image is a vital process. However, while eliminating the noise, artifacts are introduced and image blurring occurs to the MR image which is a challenging process for researchers. The spacial domain, transformed domain, and statistical property signal manipulation techniques are all covered by the denoise filtering techniques. In the spatial domain, filtering reduces noise by averaging pixels (Ali 2018).

The filtering techniques can be generally characterized as spatial and frequency domain. In-depth discussion on segmentation, wavelet-based de-noising, and linear and non-linear filtering techniques. The wiener, weighted median, adaptive, hampel, and the proposed AFHI filtering techniques for image denoising are covered in detail in the ensuing subsections. The sample images before pre-processing are listed annexure I and II. In this study, these filtering processes are performed prior to giving them as inputs to the pre-trained CNN learning model.

4.2.1 Wiener Filter

Wiener filter is used to reduce the noise that has distorted an image and produces results that are identical to the first image. The goal is to have the smallest amount of mean square error possible. The earlier knowledge of the noise in an image is investigated by 3 Adaptive FilterWiener filtering. It has the capability of wide-ranging rebuilding for locating the loud image. Figure 4.1 shows the de-noised images using Wiener filter on ADNI and OASIS datasets.

Stage	Noisy ADNI dataset images	Wiener Filter on ADNI dataset	Noisy OASIS dataset images	Wiener Filter on OASIS dataset
Normal			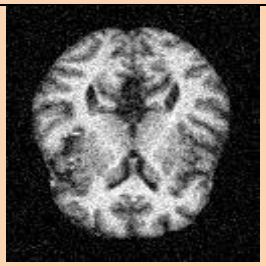	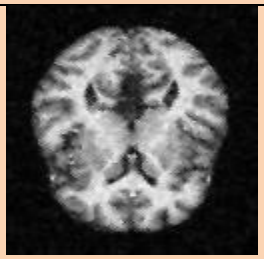
Stage 1	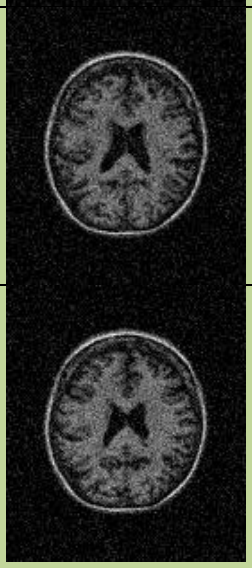		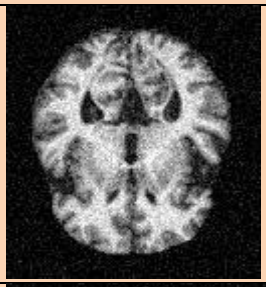	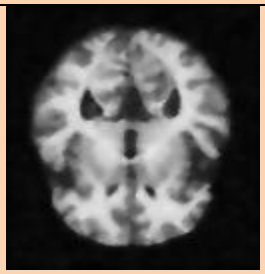
Stage 2			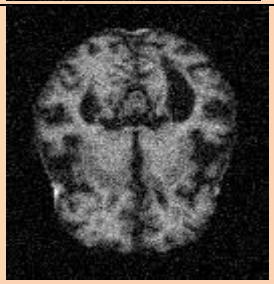	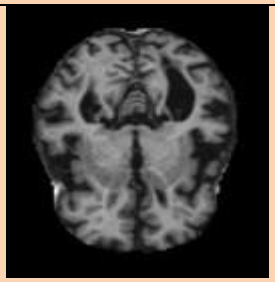
Stage 3	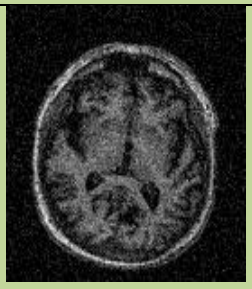	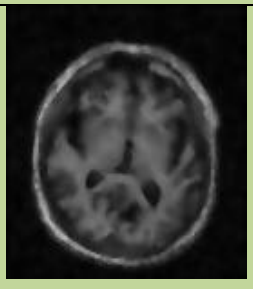		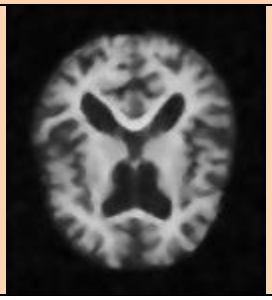

Figure 4.1 Denoised brain neuron MR images using the Weiner filter on ADNI and OASIS Datasets

4.2.2 Weighted Median Filter

It takes a filter window for each pixel and calculates the median of a neighboring pixel. The center pixel is replaced by this value like average filter that averages all the filter window pixels. The edges are protected with high frequency components of an image that is impossible with an average filter. This filter effectively and robustly reduces noise in signal processing. The original pixel in median filter results gives an output of same pixel known as root mask. All of the signals here converge to the root signal. By blurring the impulse noises, the filter decreases them, which causes some details in the image to be lost.

The Weighted Median filter smoothers are heavily limited because they can only accept positive weights and are essentially smoothers with "lowpass" type filtering properties. Numerous engineering applications demand frequency filtering qualities with "bandpass" or "highpass" characteristics. For example, outputs from linear FIR equalisers that accept only positive filter weights would be wholly undesirable. These undesirable results are produced by weighted median smoothers that only accept positive weights. As the sample mean may be generalized to the rich class of linear FIR filters, the median can logically be generalized to a rich class of weighted median filters that admit both positive and negative weights. Figure 4.2 shows the denoised images using weighted median filter on ADNI and OASIS datasets.

Stage	Noisy ADNI dataset images	Weighted Median Filter on ADNI dataset	Noisy OASIS dataset images	Weighted Median Filter on OASIS dataset
Normal			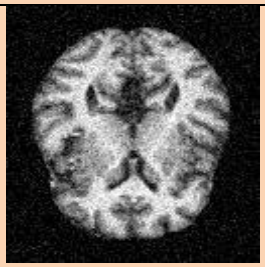	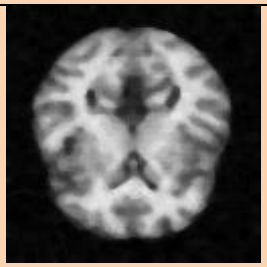
Stage 1			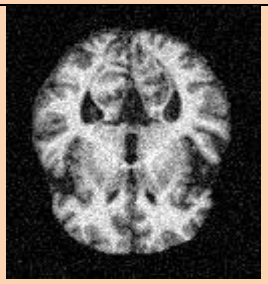	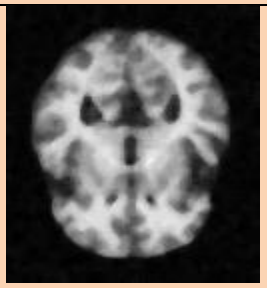
Stage 2			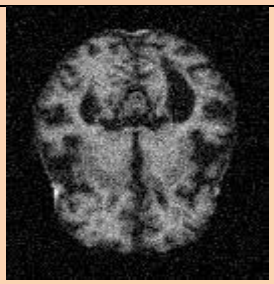	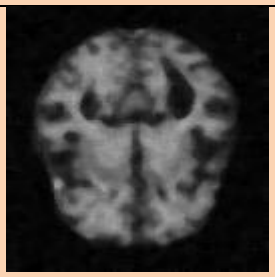
Stage 3	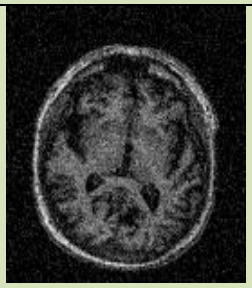	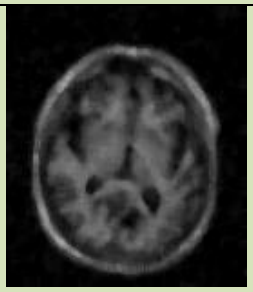	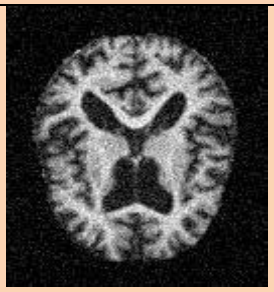	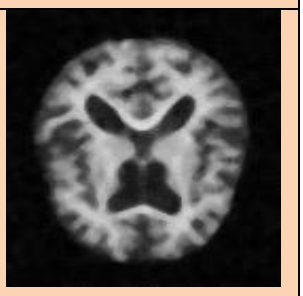

Figure 4.2 Denoised brain neuron MR images using the Weighted Median filter on ADNI and OASIS Datasets

4.2.3 Adaptive Filter

The window size is altered and the edges are preserved to achieve good results in adaptive filter technique. The output is better than any linear filters is the advantage of this filter. The image is blurred and edges are protected if high frequency sections are present in the image. The linear and nonlinear filters are used depending on their working

opinion. It is challenging to decide which filter is used depending on the situation and the image. Figure 4.3 shows the denoised images using adaptive filter on ADNI and OASIS datasets.

Stage	**Noisy ADNI dataset images**	**Adaptive Filter on ADNI dataset**	**Noisy OASIS dataset images**	**Adaptive Filter on OASIS dataset**
Normal			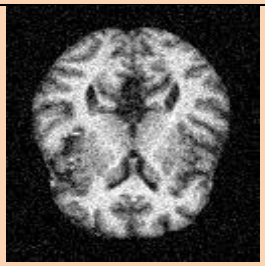	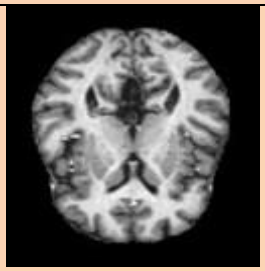
Stage 1	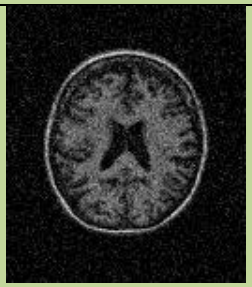		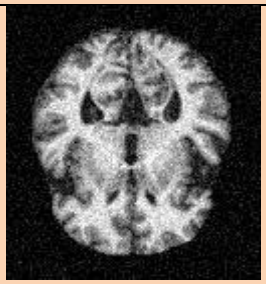	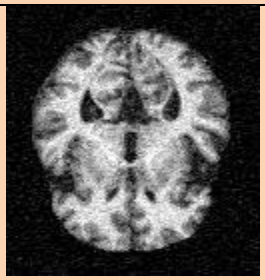
Stage 2			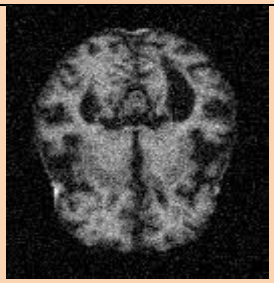	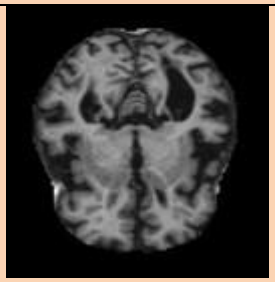
Stage 3	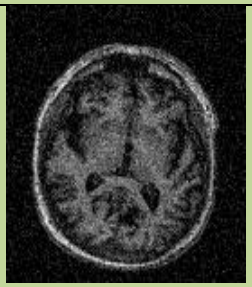	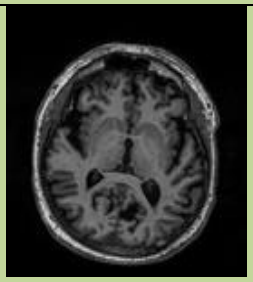	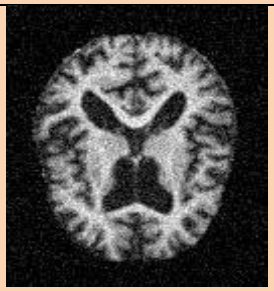	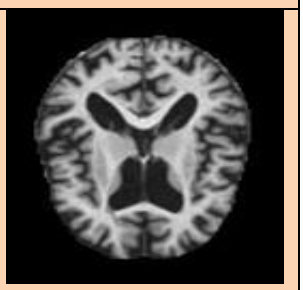

Figure 4.3 Denoised brain neuron MR images using the Adaptive filter on ADNI and OASIS Datasets

4.2.4 Hampel Identifier Filter

The position and dispersion of the outliers are estimated using the median and median absolute deviation. The latter is used to estimate the standard deviation of the data and to find outliers, while the former is used to estimate the data location. Figure 4.4 shows the denoised images using Hampel identifier filter on ADNI and OASIS datasets.

Stage	Noisy ADNI dataset images	Hampel Identifier filter ADNI dataset	Noisy OASIS dataset images	Hampel identifier filter on OASIS dataset
Normal	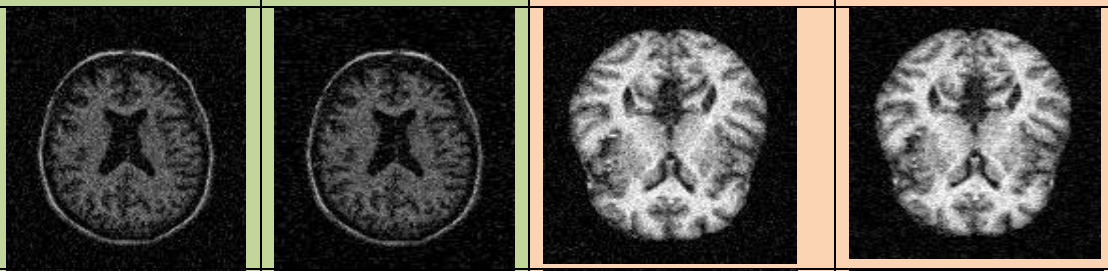			
Stage 1				
Stage 2				
Stage 3				

Figure 4.4 Denoised brain neuron MR images using the Hampel identifier filter on ADNI and OASIS Datasets

4.2.5 Proposed Hybrid AFHI Method

In this study the brain images of the AD patient is used to effectively de-noise the MRI. The AFHI method's initial contribution effectively manages different Gaussian noise levels in the grayscale images. Removal of noise from the image is performed without any loss of features such as spatial and edges. The smoothening effect is produced in the Gaussian filter. The smoothening ratio depends on the Gaussian function given in equation (4.1).

$$G_{\sigma}(i, j) = \frac{1}{2\Pi\sigma^2} e^{-\frac{(i^2+j^2)}{2\sigma^2}} \qquad (4.1)$$

Here ‘i’ and ‘j’ denotes the vertical and horizontal axis from the centre. σ denotes the distribution of standard deviation.

MRI records signals that have gradient fields are applied in three orthogonal directions to encode their frequency. In order to achieve spatial encoding, an upgraded application in a homogeneous field results in a linear variation. When metallic items with elevated magnetic exposure are placed in the magnetic field, the structural encoding mistakes result in artefacts and noise. The researchers have used a noise filtering methods to decrease the noise. This study focuses on eliminating the noise and artefacts with random values while preserving fine features. Figure 4.5 shows the de-noised images using proposed hybrid AFHI method on ADNI and OASIS datasets.

Stage	Noisy ADNI dataset images	Proposed hybrid AFHI method on ADNI dataset	Noisy OASIS dataset images	Proposed hybrid AFHI method on OASIS dataset
Normal			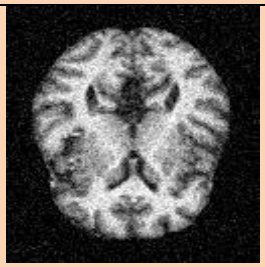	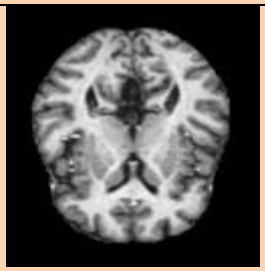
Stage 1	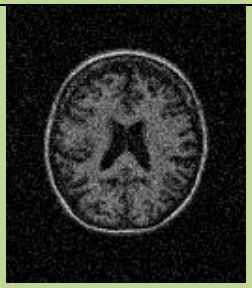		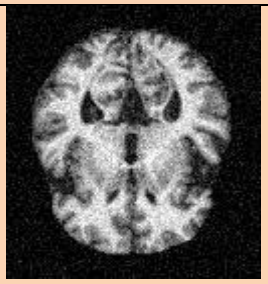	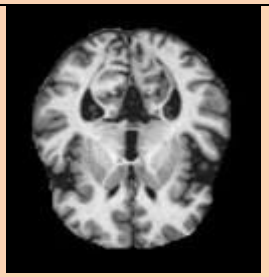
Stage 2			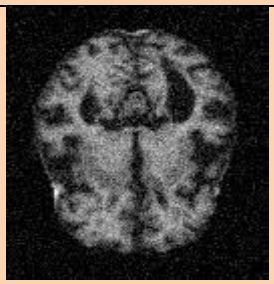	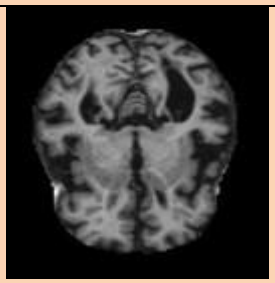
Stage 3	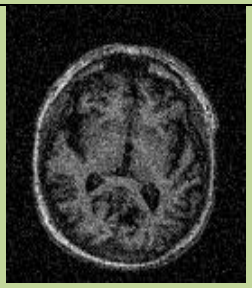	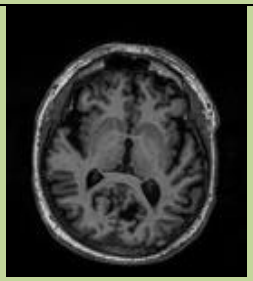	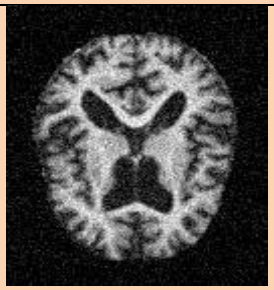	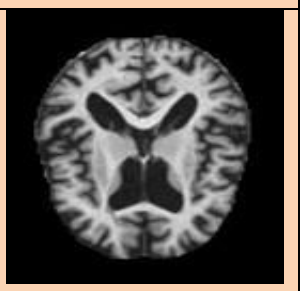

Figure 4.5 Denoised brain neuron MR images using the proposed hybrid AFHI method on ADNI and OASIS Datasets

4.2.5.1 Performance Evaluation of the hybrid AFHI method

The wiener, weighted median, adaptive and hampel are examined and contrasted with the hybrid AFHI approach. Figure 4.6 (a) original noisy image and Figure 4.6 (b) denoised image obtained by the hybrid AFHI method for the ADNI dataset. Figure 4.7 (a)

and (b) display the original noisy and the denoised image obtained by the hybrid AFHI method for the OASIS.

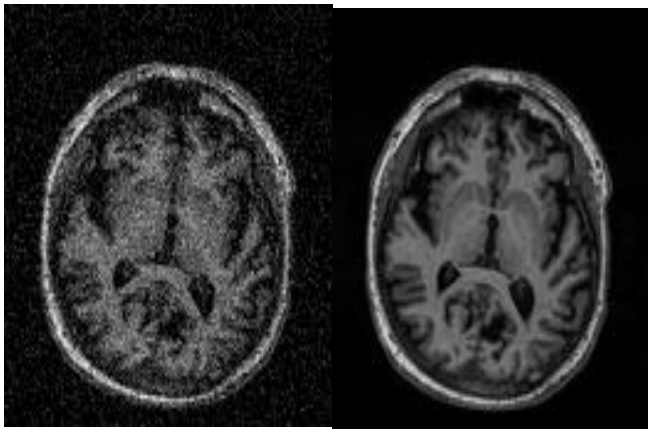

(a) (b)

Figure 4.6 (a) Original noisy image (b) Denoised image with stage 3 by proposed hybrid AFHI method on ADNI Dataset

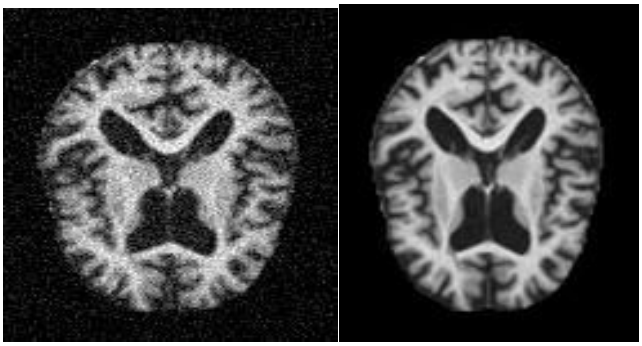

(a) (b)

Figure 4.7 (a) Original noisy image (b) De-noised image with stage 3 by proposed hybrid AFHI method on OASIS Dataset

The hybrid AFHI method's performance is evaluated using three metrics: RMSE, PSNR, and SSIM. The mathematical formulation for calculating the RMSE and PSNR values is represented in equations (4.2) and (4.3).

$$RMSE = \frac{1}{M_1 x M_2} \sum_{i=1}^{M_2} \sum_{j=1}^{M_1} [I(i, j) - I'(i, j)]^2 \quad (4.2)$$

$$PSNR = 10\ x \log(\frac{255^2}{RMSE}) \quad (4.3)$$

where I and I' denotes two images M1×M2 size. The pixel value of the i^{th} row and j^{th} column of I and I' represents I(i,j) and I'(i,j). The estimation of SSIM values is shown in equation (4.4).

$$SSIM(I,I') = \frac{(2\mu_I\mu_{I'} + c_1)(2\sigma_{II'} + c_2)}{(\mu_I^2 + \mu_{I'}^2 + c_1)(\sigma_I^2 + \sigma_{I'}^2 + c_2)} \quad (4.4)$$

where $\mu_I = \sum_{i=1}^{N} w_i x_i$ and $\sigma_I = \left(\sum_{i=1}^{N} w_i (x_i - \mu_I) \right)^{1/2}$ denotes average grey value and I variance. $\sigma_{II'} = \sum_{i=1}^{N} w_i (x_i - \mu_I)(y_i - \mu_{I'})$ denotes the covariance between I and I'. $C_1 = (K_1 L)^2$ and $C_2 = (K_2 L)^2$ denotes the two constants.

Figure 4.8 represents the RMSE performance measure analysis of ADNI and OASIS datasets obtained by wiener, weighted median, adaptive, hampel, and the proposed AFHI methods. The proposed AFHI method outperforms the other techniques on ADNI and OASIS datasets. RMSE values of ADNI dataset 0.23 and OASIS dataset is 0.3.

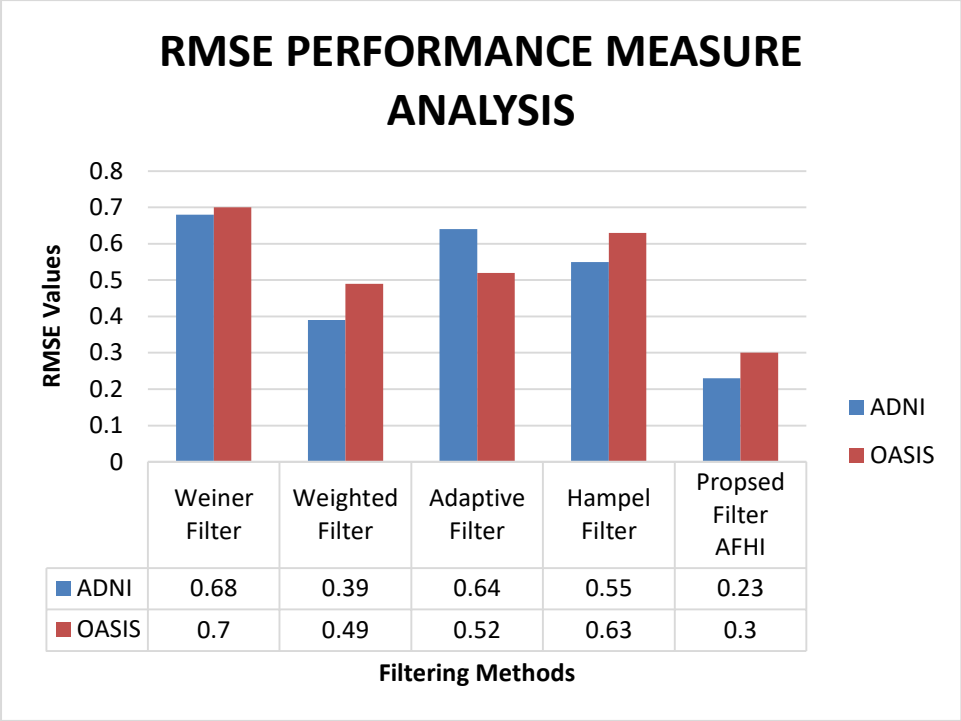

	Weiner Filter	Weighted Filter	Adaptive Filter	Hampel Filter	Propsed Filter AFHI
ADNI	0.68	0.39	0.64	0.55	0.23
OASIS	0.7	0.49	0.52	0.63	0.3

Figure 4.8 RMSE Performance measure analysis of filtering methods for ADNI and OASIS datasets

Figure 4.9 represents the PSNR performance measure analysis of ADNI and OASIS datasets obtained by wiener, weighted median, adaptive, hampel, and the hybrid AFHI method. PSNR values obtained by the hybrid AFHI method on ADNI and OASIS datasets are 30.05 decibel and 29.88 decibel, respectively. The AFHI method overhauls the other methods on ADNI and OASIS by obtaining the maximum PSNR value equated to the other methods.

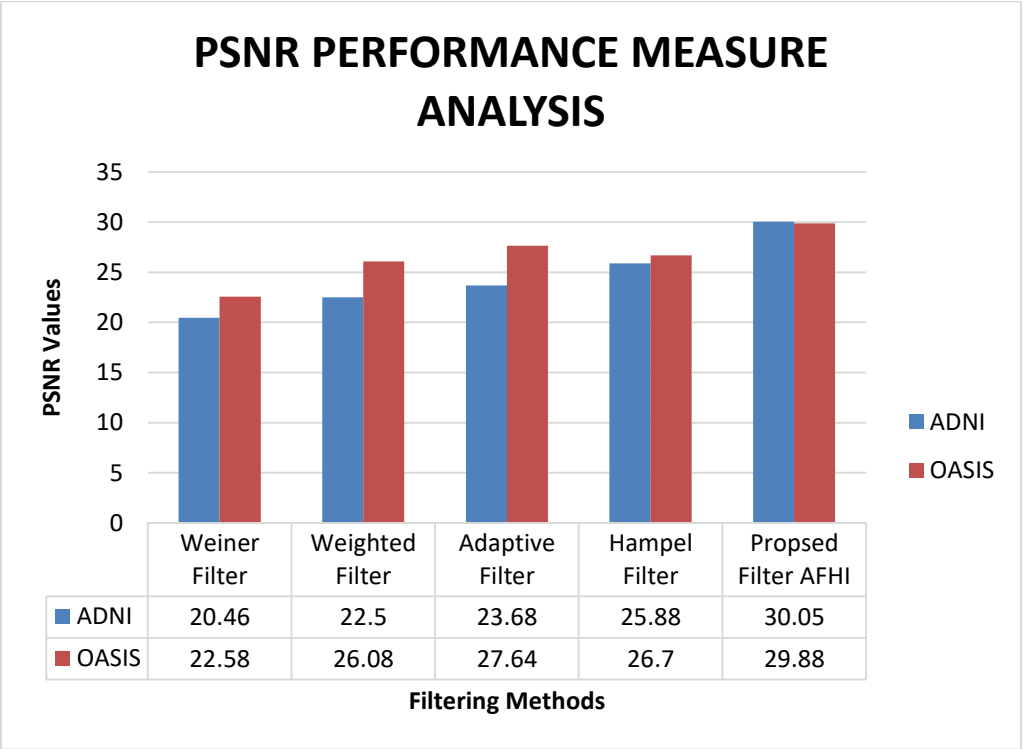

	Weiner Filter	Weighted Filter	Adaptive Filter	Hampel Filter	Propsed Filter AFHI
ADNI	20.46	22.5	23.68	25.88	30.05
OASIS	22.58	26.08	27.64	26.7	29.88

Figure 4.9 PSNR Performance measure analysis of Filtering methods for ADNI and OASIS datasets

Figure 4.10 represents the Structural Similarity Index Means (SSIM) performance measure analysis of ADNI and OASIS datasets obtained by wiener, weighted median, adaptive, hampel, and the hybrid AFHI method. SSIM obtained by the hybrid AFHI method on ADNI and OASIS datasets are 0.95 and 0.9. The AFHI method beats the others on ADNI and OASIS by obtaining the maximum SSIM value equated to the other methods.

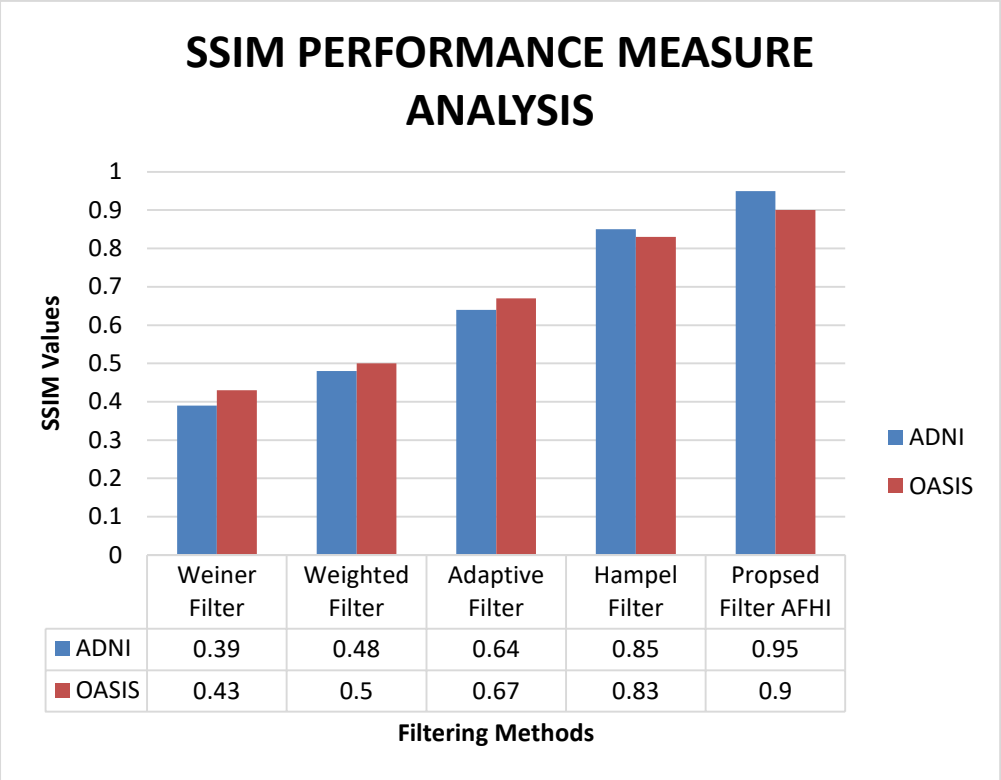

Figure 4.10 SSIM Performance measure analysis of filtering methods for ADNI and OASIS datasets

4.3 Segmentation Techniques

After de-noising, segmentation is performed on the AFHI filtered brain neuron image for effective skull stripping operation. Techniques like region growing technique, histogram based thresholding in DWT, and FCM clustering are applied. The proposed hybrid segmentation technique named TDWT_FST performs fuzzy edge detection and morphological operations.

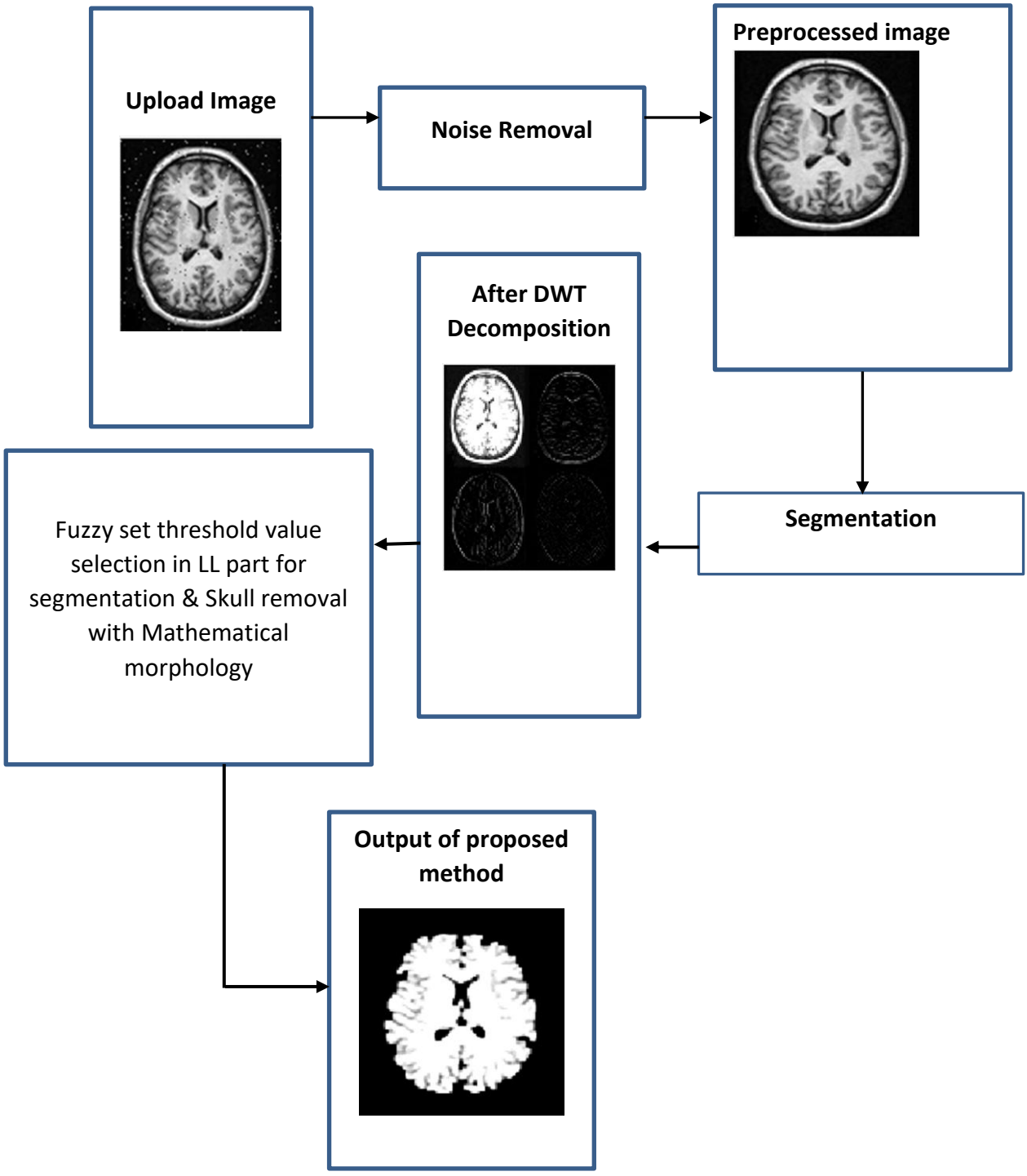

Figure 4.11 Proposed architecture for segmentation

4.3.1 Region growing technique

Region growth is an image segmentation technique that relies on choosing key seed points and then including neighboring pixels area according to conditions, like intensity value or color similarity. Image is separated into background and foreground regions, by using this algorithm. Let x∈I represent a randomly selected pixel in an input 2D digital image. Let R_f stand for the input picture I's ROI (Region Of Interest). The acceptance of the shift in intensity value is indicated by the foreground δ_1. Compare each neighboring pixel to the primary seed to increase ROI, and if it succeeds, assign all pixels to R_f.

$$|x\text{-}N(p)| \leq \delta\_1 \tag{4.5}$$

where x represents N(p) ∈ I's neighborhood pixel. The neighboring pixel is computed similarly when the pixel is assigned to R_f. If it is assigned wrongly, a noisy pixel will be selected as the result. Comparing the pixel with the furthest region to the neighboring pixel is an additional method. N(p) and the farthest pixel of R_f are being compared here.

$$|S(x)\text{-}N(p)| \leq \delta\_1 \tag{4.6}$$

Here, a single pixel cannot begin the initialization process. A small pixel group larger than the region is required to describe the region using mean or variance tools. Here, an exclusive process happens when each adjacent pixel is analyzed throughout the full area. The various steps involved are given below:

STEP 1: Read image 'I'.

STEP 2: Select image 'I' and its seed pixel 'x'

STEP 3: Verify the adjacent image pixels' 'N(p)'. Put the same seed value into R_f.

STEP 4: For each newly added pixel, repeat "step 2." Finally, stop when there is no more pixels available to insert.

The startup process is started by specifying the seed point. Images that choose an unsuitable initial seed point are either over- or under-segmented. When utilizing the RG method, FEIs are occasionally typically endured with low resolution, minimized contrast, and speckle noise, leads to disjointedness.

4.3.2 Histogram based thresholding

Depending on the parameters of the input image, the threshold approach is used for object segmentation. It occurs in pictures where a light object is consumed by a dark background, or the other way around. The objects are detached from the background using thresholding technique, and a suitable threshold value is chosen to separate the pixels in the image using specific classes. Any pixel (x, y) with value f(x, y) <T is estimated as background, and an input image with pixels f(x, y)>=T is estimated as foreground.

When the intensity sharing between the foreground and background objects is highly different and a single threshold value can be used to easily distinguish both objects independently. The attributes determine the image's gray level value and its threshold value T. Entropy and the Otsu method are examples of generalized threshold methods that can be used.

4.3.3 Proposed TDWT-FST Technique for segmentation

Accurately segmenting the brain while preserving the AD-MRI details is the ultimate goal of the proposed system. For an object segment in MRI, there were other models available; however, because it incorporates the threshold system, the suggested model is thought to be more effective. Figure 4.11 shows the working of proposed TDWT-FST technique. MRI system depends on the storing/recording of signals, which are frequency encoded by using gradient fields applied in 3 orthogonal directions. To make spatial encoding, the application of an incline in a homogeneous part produces a linear variation. It is linear in a similar magnetic field for each spatial coordinate of the studied volume, resembling a single frequency synchronization. Artifacts and noises are generated by spatial encoding errors when high magnetic susceptibility is placed within

the magnetic field. The goal of this study is to remove random valued artifacts and noise without sacrificing fine details.

To eliminate noise and artifacts, an Adaptive Hampel Identifier (AHI) elimination method is suggested. Identify window is used to convert 1D to 2D is clearly derived from image processing systems. The following is a description of the suggested algorithm:

Input: noisy image $Y \in R^{MxN}$

For each pixel $x_m(n)\ in\ Y\ do$

Estimate median $\mu_m(n) = med\{F_W(x_m(n))\}$ and median absolute deviation $\sigma_m(n) = 1.4826.med\{A(|\ x_m(n)\ |)\}$ (4.7)

Where $x_m(n)$ specifies element located at m[th] row and n[th] column of X, 2W +1 represents sample window.

Calculate the adaptive rejection threshold $\Gamma = \dfrac{c}{win_{\max} - win_{\min} + \varepsilon_1}$

Where c denotes the gray scale image with value of 256, $\varepsilon_1 > 0$ denotes positive constant, $win_{\max}$ represent maximum detect window and $win_{\min}$ represent the maximum window.

$win_{\max} = \max Fw(x_m(n))$ and $win_{\min n} = \min Fw(x_m(n))$ (4.8)

4.3.3.1 Discrete Wavelet Transform (DWT)

DWT is a tool to splits 2D image histogram into multiple scales based on 'T' threshold value. To segment the object 'T' is used by relying on DWT in order to prevent noise. The input MRI is decomposed into different wavelet coefficient levels.

The input image consists of low and high frequency parts, that gives global information about the data. The filtering process is achieved with high scale and low frequency of the image components. An input image is sub-sampled into several frequency modules and bands. Here, the input images are deconstructed by running them through high pass and low pass filters, with L representing low pass & H representing

high pass. A series of filters are then created, including low pass (LL), high pass (LH), low pass (HL), and high pass (HH). Up until an input MRI is deconstructed to a predetermined reference level, this process can be repeated. Figure 4.12 shows the DWT processing structure.

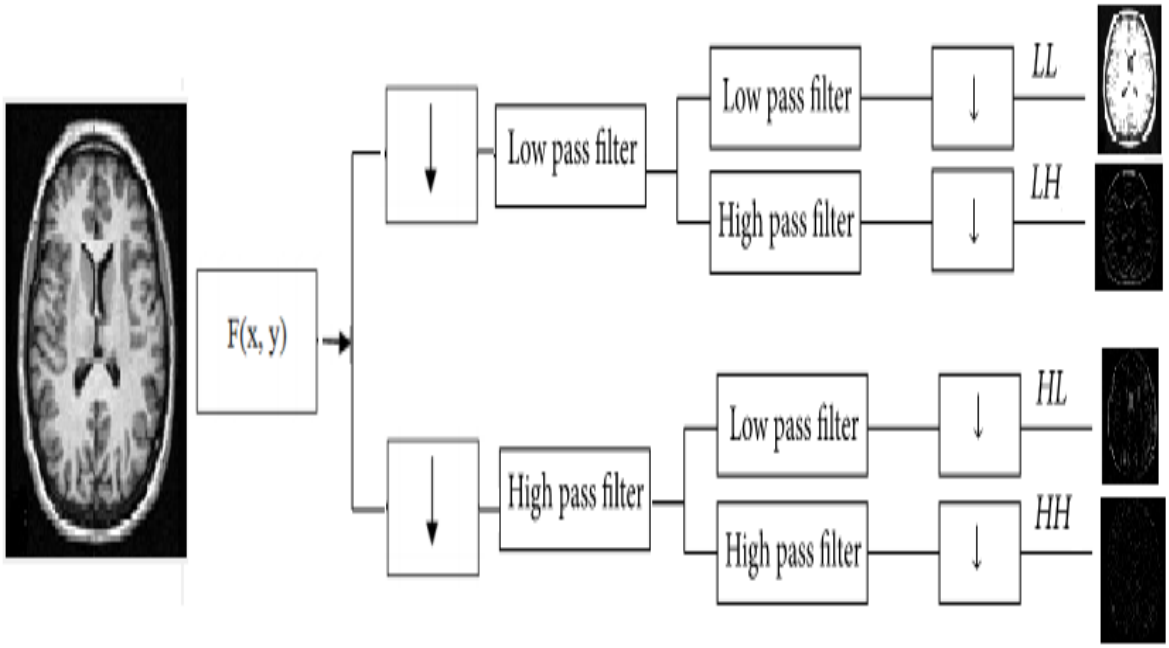

Figure 4.12 DWT processing structure

Four subband images generated from MRI are shown in Figure 4.12. In this case, HH is extremely susceptible to noise, HL varies with changes in position, and LH is sensitive to variances in expression. Wavelet consist of a decomposition filters and arbitrary molded waveform. This work uses a Haar-based wavelet for decomposition. The output image's ↓ indicates that all down-sampled columns, including indexed columns, have been chosen. Complex low-pass and high-pass filters are used to create the output images. Following convolution, down sample the images using rows by designating ↓, which eventually produces four subband images. Finally, different types of sub-band images are produced, which include horizontal, vertical, and diagonal information of the image. Thus, the four sub-band images are generated consisting of the horizontal, vertical, and diagonal details. If the image includes 2k elements in the column or row, then k low pass as well as k high pass wavelet transform constants will be created

after every level of filtering process. The equations of filter analysis are presented in below equations. The low pass filters and high pass filters are given in (4.9) and (4.10).

$$h(k) = x(2k) + (g(k-1) + g(k)/8) \tag{4.9}$$

$$g(k) = 2.x(2k+1) - x(2k) - x(2k+2) \tag{4.10}$$

In this case, x(k) denotes pixel value at k^{th} location, g(k) specifies k^{th} high pass coefficient, and h(k) specifies k^{th} low pass coefficient. The approximation coefficient, or LL, contains the majority of the image's details. For the following steps, such as object segmentation and mathematical morphological operations for skull exclusion, the LL component is selected.

4.3.3.2 Fuzzy set c-means clustering

Let 'A' denote an input image, with M × M size, with L gray levels where 'μA(aij), 0 ≤ μA(aij) ≤1' denotes membership value of '$(i,j)^{th}$' pixel in input image A. Exactly the fuzzy image can be denoted as 'A ={aij, μA(aij)}'. In the provided image, let the count' (f)' represent an instance count of the gray level 'f' [13]. Equation (4.11) provides average gray level of the background region and the object region, based on a specific threshold value 't' that splits object and the background.

$$\mu_0 = \frac{\sum_{f=0}^{t} f.count(f)}{\sum_{f=0}^{t} count(f)}$$

$$\mu_1 = \frac{\sum_{f=t+1}^{L-1} f.count(f)}{\sum_{f=t+1}^{L-1} count(f)} \tag{4.11}$$

A section of the image's pixel membership value is determined by how appealing that region fits. The Gamma distribution function has been used to determine the image pixels' membership values. The equation (4.12) mentioned the common form of Gamma distribution,

$$f(x) = \frac{\left(\frac{(x-\mu)}{\beta}\right)^{\gamma-1} \exp\left(-\frac{x-\mu}{\beta}\right)}{\Gamma(\gamma)}, x \geq \mu, \gamma, \beta > 0 \qquad (4.12)$$

Here, γ stands for shape, μ for position, β for scale, and Γ for the Gamma function. The Gamma distribution in equation (4.12) looks like this if μ ≠0, β = 1, and γ = 1:

$$f(x) = \exp[-(x-\mu)] \; as \; \Gamma(1) = 1 \qquad (4.13)$$

By choosing μ = μ1, the object's average gray level region is displayed as follows: μA(aij) represents the object region's membership function for a particular image and is estimated using equation (4.13).

$$\mu_A(a_{ij}) = \exp(-c.|a_{ij} - \mu_1|) \; if \; a_{ij} > t \qquad (4.14)$$

Similarly, Let μ=μ0, background region's average gray level is provided in (4.15), the background region membership function, represented by μA(aij), may be computed using equation (4.14).

$$\mu_A(a_{ij}) = \exp(-c.|a_{ij} - \mu_0|) \; if \; a_{ij} \leq t \qquad (4.15)$$

where 'c' stands for constant in [0, 1]. In this case, 'c' selects 'c = 1/(□max -□min)', where '□min' and '□max' represent low and high gray levels of image. To estimate membership function, distance between the pixel's gray level and object region's mean to which it fits has been measured.

4.3.3.3 Mathematical Morphology

Skull stripping in brain MRI refers to the removal of tissues that are not part of the brain. The shape-based tool Mathematical Morphology (MM) is applied to extract components like region, shape description, boundaries and convex hull. Set theory is used to develop the MM tool. MM aims to examine an input image's morphological structure by applying specific patterns, referred to as Structuring Elements (SE), at various points

on the image. A small pixel connected component that is utilized to obtain the essential morphological data from the given images using SE components.

Erosion and dilation are the significant basic operations in MM which also used to derive some other operations such as opening, closing. Erosion and dilation are applied appropriately to reduce and enlarge the image's elements.

Let "A" stand for the input binary image set and "S" for "SE" in "Z2." The erosion of A by S is represented by A□S, as seen below:

$$A\theta S = \{z \mid (S)_z \subseteq A\} \tag{4.16}$$

Pixel set 'S' located at that pixel is limited within A, and this is known as the Erosion of A by the S, or A□S. All points set 'z' in S is the erosion. Erosion reduces an object's form and is used to remove small, annoying things from an input image. A⊕S is the expansion of "A" using "S" in "Z2." Enlargement of A using S and all movements group is denoted by a single component as shown below:

$$A \oplus S = \{z \mid (S)_z \cap A \neq \phi\} \tag{4.17}$$

Enlargement is utilized for enriching an output image. It emphasizes image's slight objects. In MM, the opening action produces a smoothed object's shape with a break in the thin lines, while the closing operation smoothes the contours and often eliminates tiny gaps in the objects. With 'A' standing for the image and S for SE, the symbols A○S and A●S, respectively, indicate opening and closing operations. Dilation is used to compute erosion in opening, while erosion is used to calculate dilation in closing.

Opening, $A \circ S = (A\theta S) \oplus S)$

Closing, $A \bullet S = (A \oplus S)\theta S)$ (4.18)

The morphological reconstruction is performed in the main operation to extract associated components in the input image. The morphological reconstruction is developed through a sequence of dilation operations until the marker image edge fits beneath a second image, known as mask image. Skull stripping is a crucial process in brain MRI analysis. It eliminating the non-cerebral tissues like skull, meninges also eyeball from the

MRI. Figure 4.13 compares the original denoised brain neuron images with region growing, histogram-based thresholding and proposed TDWWT-FST techniques using ADNI dataset. Figure 4.14 compares the original denoised brain neuron images with region growing, histogram-based thresholding and proposed TDWWT-FST techniques using OASIS dataset.

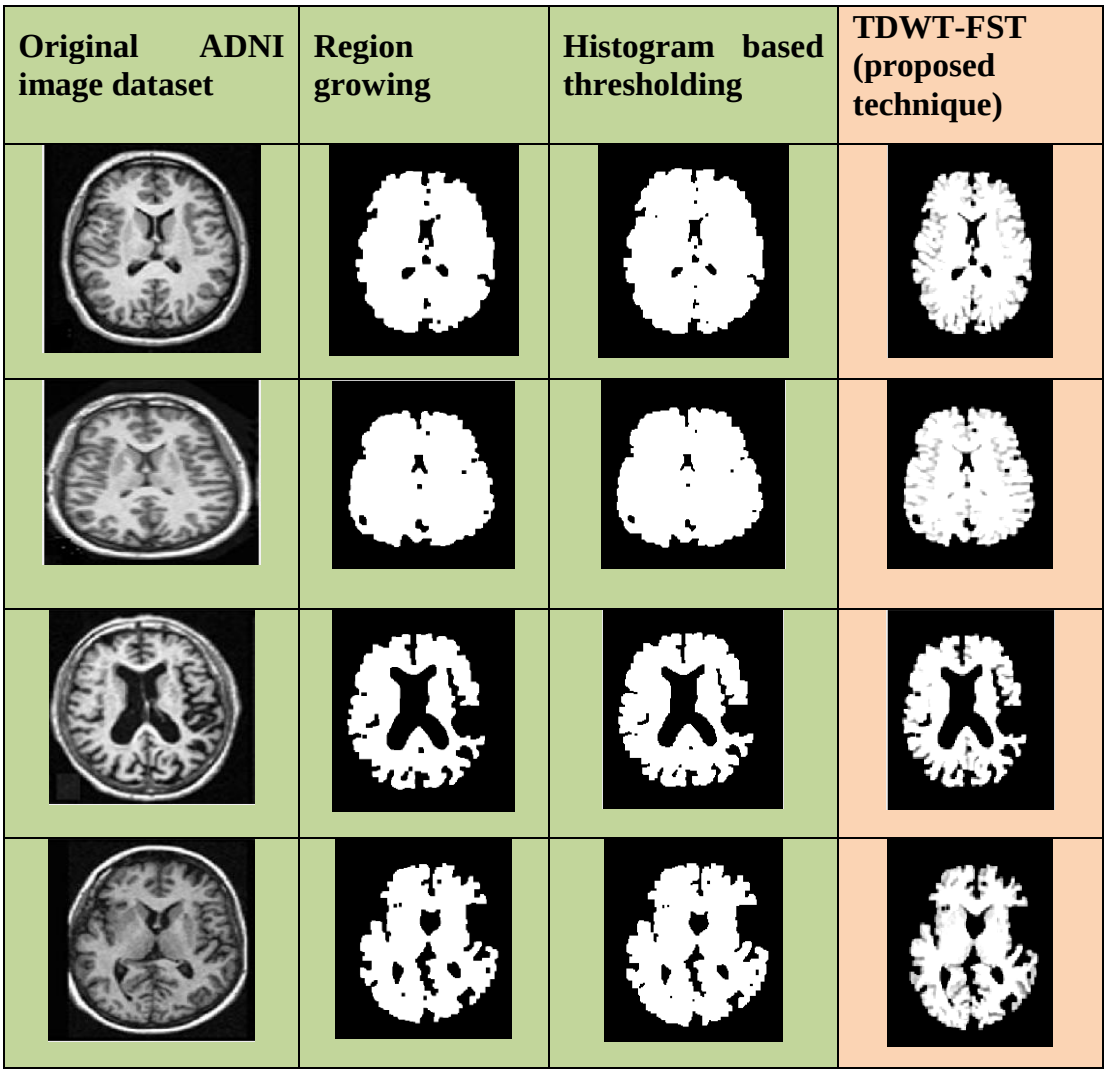

Figure 4.13 Comparison of denoised brain neuron MR images using ADNI Datasets

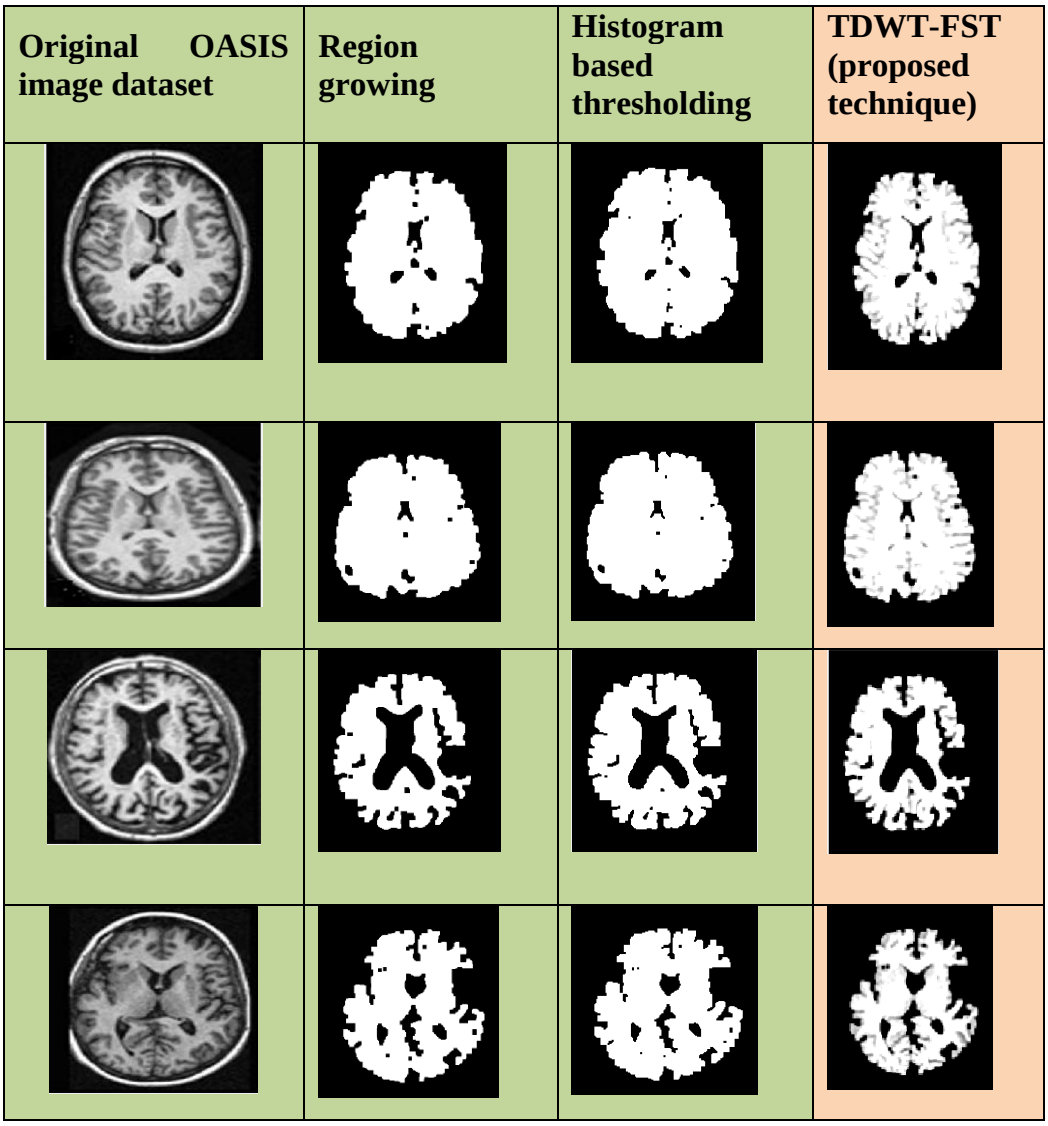

Figure 4.14 Comparison of denoised brain neuron MR images using OASIS Datasets

The performance metrics of TDWT-FST approach is evaluated using Mean Absolute Error (MAE), PSNR, and RMSE. MAE is an amount useful to recognize nearness of predictions are to the latest outcomes. The MAE is given by equation (4.19)

$$MAE = \frac{1}{mn} \sum_{i=1}^{m} \sum_{j=1}^{n} \left(f_{i,j} - y_{i,j} \right) \qquad (4.19)$$

Here, $f_{i,j}$is the original image and $y_{i,j}$ is the evaluated image. i = 1, 2.., M (range index) and j = 1, 2.., N (cross-range index).

Figure 4.15 represents the RMSE performance measure analysis for ADNI and OASIS datasets obtained by Region Growing, histogram-based thresholding and the proposed TDWT-FST methods. The proposed TDWT-FST method outperforms the other techniques on ADNI and OASIS datasets. The RMSE values of ADNI dataset 0.38 and OASIS dataset is 0.42.

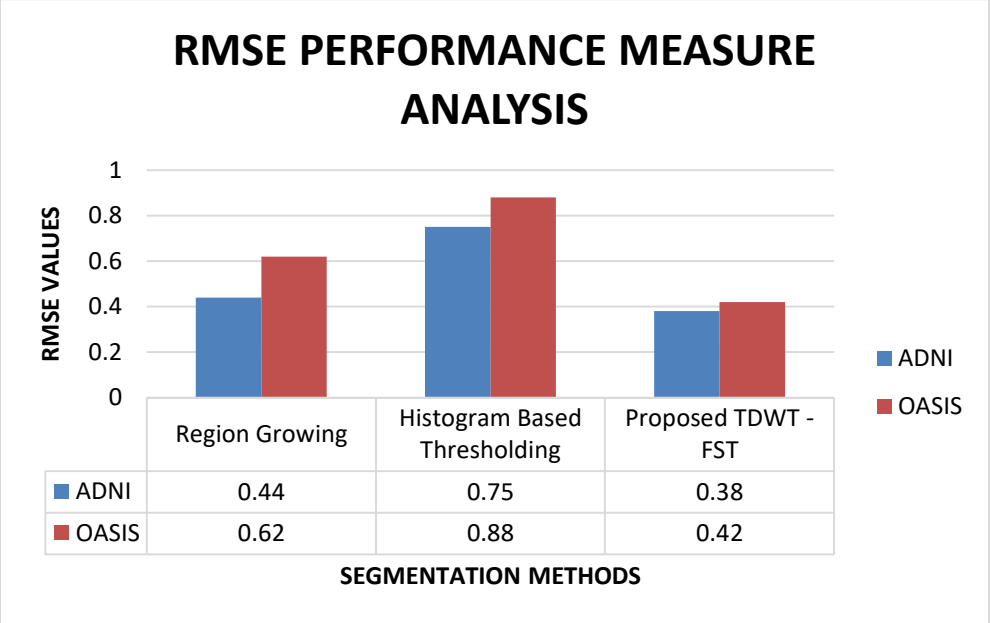

Figure 4.15 RMSE Performance measure analysis of segmentation methods for ADNI and OASIS datasets

Figure 4.16 represents the PSNR performance measure analysis of ADNI and OASIS datasets obtained by region growing, histogram-based thresholding and the proposed TDWT-FST methods. The PSNR values obtained by the proposed TDWT-FST method on ADNI and OASIS datasets are 56.28 decibel and 58.03 decibel, respectively. The TDWT-FST method overtakes the other methods on ADNI and OASIS by obtaining the maximum PSNR value equated to the other methods.

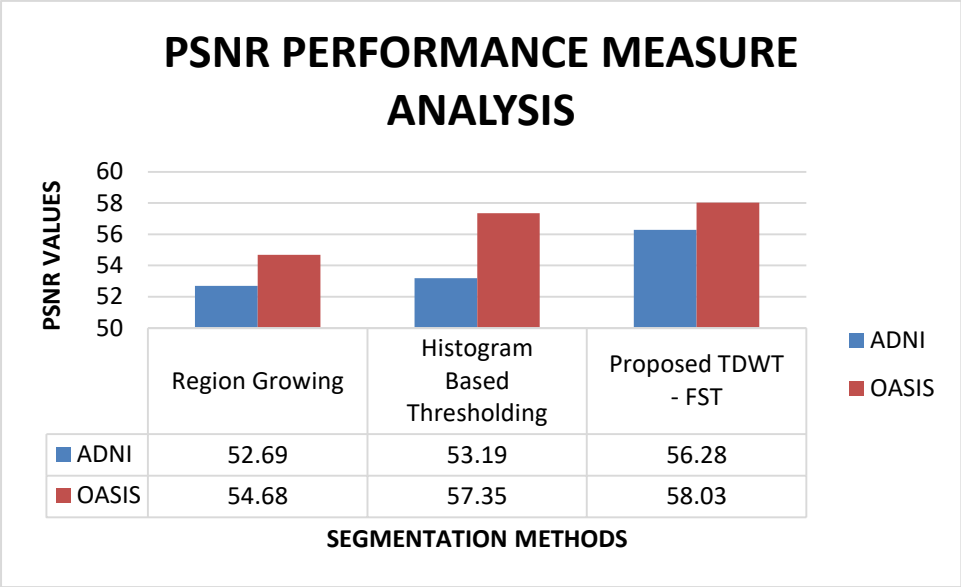

Figure 4.16 PSNR Performance measure analysis of segmentation methods for ADNI and OASIS datasets

Figure 4.17 represents the MAE performance measure analysis of ADNI and OASIS datasets obtained by region growing, histogram based thresholding and the proposed TDWT-FST methods. The proposed TDWT-FST method outperforms the other techniques on ADNI and OASIS datasets. The MAE values of ADNI dataset 0.36 and OASIS dataset is 0.35.

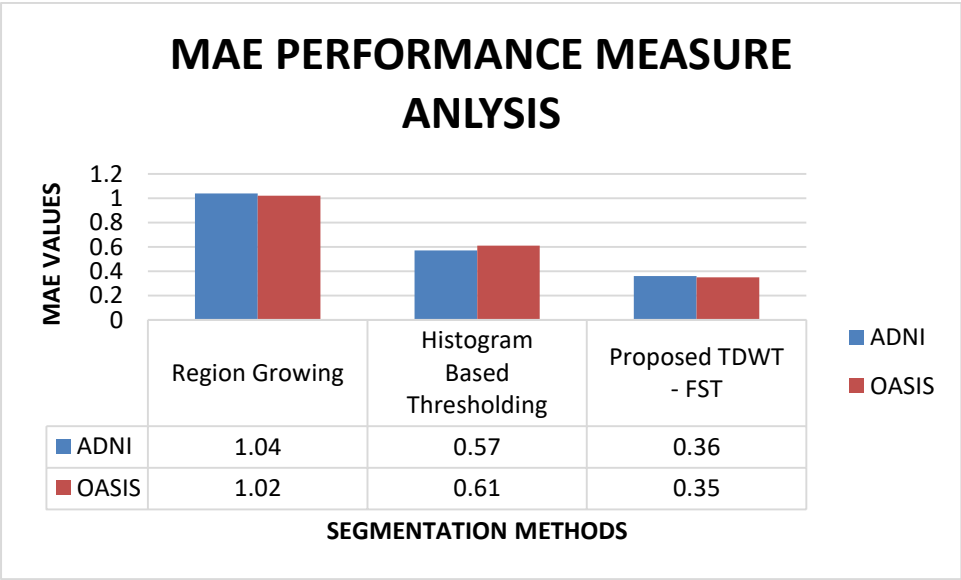

Figure 4.17 MAE Performance measure analysis of segmentation methods for ADNI and OASIS datasets

4.4 Summary

This chapter applied a variety of image preprocessing techniques to the brain neuron image in order to remove image noise. Datasets from OASIS and ADNI are used for evaluation. A description is given on image preprocessing methods, including the weighted median, adaptive, hampel, wiener, and the suggested AFHI methods for image denoising. A study on filtering techniques is performed, and the test results show that the values produced by the AFHI method overtakes the other filtering methods. The AFHI approach is assessed in this study using performance metrics such as RMSE, PSNR, and SSIM. Image segmentation techniques such as region growing, histogram-based thresholding and the proposed TDWT-FST methods are applied for segmentation. The segmentation techniques are evaluated on both datasets using performance metrics like RMSE, PSNR, and MAE. In this study, the proposed AFHI and TDWT-FST methods efficiently preprocesses the images on ADNI and OASIS datasets are presented.